



Article

Induction of Innate Memory in Human Monocytes Exposed to Mixtures of Bacterial Agents and Nanoparticles

Giacomo Della Camera^{1,2}, Tinghao Liu^{3,4}, Wenjie Yang^{3,4}, Yang Li^{3,4} , Victor F. Puentes^{5,6,7}, Sabrina Gioria² , Paola Italiani^{1,8,9} and Diana Boraschi^{1,3,4,8,9,*}

- ¹ Institute of Biochemistry and Cell Biology (IBBC), National Research Council (CNR), 80131 Napoli, Italy
 - ² European Commission, Joint Research Centre (JRC), 21027 Ispra, Italy
 - ³ Shenzhen Institute of Advanced Technology (SIAT), Chinese Academy of Sciences (CAS), Shenzhen 518055, China
 - ⁴ China-Italy Joint Laboratory of Pharmacobiotechnology for Medical Immunomodulation (CNR, SIAT, SZN), SIAT, CAS, Shenzhen 518055, China
 - ⁵ Institut Català de Nanociència i Nanotecnologia (ICN2), Consejo Superior de Investigaciones Científicas (CSIC) and The Barcelona Institute of Science and Technology (BIST), 08036 Barcelona, Spain
 - ⁶ Vall d'Hebron Research Institute (VHIR), 08035 Barcelona, Spain
 - ⁷ Institució Catalana de Recerca i Estudis Avançats (ICREA), 08193 Barcelona, Spain
 - ⁸ Stazione Zoologica Anton Dohrn (SZN), 80121 Napoli, Italy
 - ⁹ China-Italy Joint Laboratory of Pharmacobiotechnology for Medical Immunomodulation (CNR, SIAT, SZN), IBBC, CNR, 80131 Napoli, Italy
- * Correspondence: diana.boraschi@itb.cnr.it



Citation: Della Camera, G.; Liu, T.; Yang, W.; Li, Y.; Puentes, V.F.; Gioria, S.; Italiani, P.; Boraschi, D. Induction of Innate Memory in Human Monocytes Exposed to Mixtures of Bacterial Agents and Nanoparticles. *Int. J. Mol. Sci.* **2022**, *23*, 14655. <https://doi.org/10.3390/ijms232314655>

Academic Editor: Yoshiro Kobayashi

Received: 30 September 2022

Accepted: 17 November 2022

Published: 24 November 2022

Publisher's Note: MDPI stays neutral with regard to jurisdictional claims in published maps and institutional affiliations.



Copyright: © 2022 by the authors. Licensee MDPI, Basel, Switzerland. This article is an open access article distributed under the terms and conditions of the Creative Commons Attribution (CC BY) license (<https://creativecommons.org/licenses/by/4.0/>).

Abstract: We assessed whether concomitant exposure of human monocytes to bacterial agents and different engineered nanoparticles can affect the induction of protective innate memory, an immune mechanism that affords better resistance to diverse threatening challenges. Monocytes were exposed in vitro to nanoparticles of different chemical nature, shape and size either alone or admixed with LPS, and cell activation was assessed in terms of production of inflammatory (TNF α , IL-6) and anti-inflammatory cytokines (IL-10, IL-1Ra). After return to baseline conditions, cells were re-challenged with LPS and their secondary “memory” response measured. Results show that nanoparticles alone are essentially unable to generate memory, while LPS induced a tolerance memory response (less inflammatory cytokines, equal or increased anti-inflammatory cytokines). LPS-induced tolerance was not significantly affected by the presence of nanoparticles during the memory generation phase, although with substantial donor-to-donor variability. This suggests that, despite the overall lack of significant effects on LPS-induced innate memory, nanoparticles may have donor-specific effects. Thus, future nanosafety assessment and nanotherapeutic strategies will need a personalized approach in order to ensure both the safety and efficacy of nano medical compounds for individual patients.

Keywords: innate immunity; innate memory; nanoparticles; bacteria; LPS; monocytes; macrophages

1. Introduction

Innate immune cells develop an innate memory that allows them to respond better to subsequent challenges [1–9]. The best-known agents that induce innate memory are infectious agents and microbial compounds. In particular, bacterial lipopolysaccharide (LPS) induces a type of memory that leads to a less potent inflammatory response to a second challenge, a mechanism aiming to protect the tissues/organs from inflammation-induced damage while affording a sufficient response level [10–16]. The main cells that can develop innate memory are mononuclear phagocytes (monocytes and macrophages) [2,10,11,17,18], as well as Natural Killer and other Innate Lymphoid Cells [5,9,19–22], although innate memory can also be observed with non-professional immune cells such as epithelial cells [23–28]. Among mononuclear phagocytes, there is evidence that monocytes are more reactive than macrophages in memory generation [29], suggesting that the main memory cells

are the effector blood monocytes (which extravasate and enter a point of inflammation in a tissue) that survive the inflammatory reaction and develop into monocyte-derived memory macrophages. Conversely, although there is evidence that naïve tissue-resident macrophages can develop memory in some circumstances [30], they may mainly act as sentinels that send alarm signals (e.g., chemokines).

The relevance of assessing the possible effects of engineered nanoparticles (NPs) on innate immunity stems from the fact that, with the explosion of nanotechnological applications, NPs are extensively produced and used in many different applications and products, which has raised concerns about their safety for human and environmental health. TiO₂ NPs are among the most produced types of NPs worldwide [31], with applications in manufacturing and construction (e.g., car tires, concrete, sports equipment), food additives, paintings and sunscreens among others [32–34]. TiO₂ NPs are generally considered safe [35,36], although their safety is currently being reconsidered [37]. CeO₂ NPs are largely used in solar cells [38], chemical mechanical planarization [39], corrosion protection [40], fuel oxidation catalysis [41], car exhaust treatment [42] and biological sensors [43]; they are also being explored for future therapeutic applications in a range of inflammation-based diseases based on their potent anti-oxidant activity [44–49]. NPs can enter the human body by different routes, mainly inhalation and ingestion but also by skin contact (if the skin is damaged) [50,51] or, in the case of nanomedical products, by injection. Some inhaled or ingested NPs have been shown to cross biological barriers (alveolar or intestinal epithelium) and reach the blood and inner tissues [52], where they can readily interact with innate immune cells, including monocytes and macrophages [31,53]. Whether NPs can be considered immunologically safe depends on many factors, including the NP's size, shape and composition and the concomitant presence of other bioactive agents (e.g., LPS), which can induce and modulate innate immune activation [54].

The direct effects of different NPs on innate immunity have been extensively studied [53,55,56], while less is known regarding their capacity to induce innate memory, although some studies have proposed that they can act as “priming” agents able to induce memory in innate immune cells [57–63]. In addition to a direct memory-inducing capacity, whether NPs may affect the generation of innate memory by microbial agents is an issue that still needs investigation. Even in the absence of a direct inflammatory effect, the capacity of NPs to induce or modulate innate memory is not only relevant in the general immunosafety evaluation of nanomaterials present in the human environment, but also in terms of the immunosafety of nanomedical products deliberately administered to patients.

To examine the generation of human innate memory, we have used an *in vitro* model that mimics the encounter between blood monocytes (representing the effector cells recruited into an inflamed tissue) and bacteria (represented by the main inflammatory molecule of gram-negative bacteria, i.e., LPS). Monocyte activation by LPS was assessed in the absence or in the presence of different types of NPs in order to examine whether NPs may have a direct effect on monocyte activation or affect LPS-induced activation. The NPs examined here include differently shaped CeO₂ (spherical, stamp-like) and seed-like TiO₂. The capacity of these NPs to directly induce innate memory or to affect the tolerance-type memory generated by exposure to LPS was assessed by examining cell activation in terms of alterations to the balance between inflammatory and anti-inflammatory cytokines.

The results obtained with these three types of NPs were compared with previously published results obtained in the same experimental conditions (endotoxin-free NPs pre-coated with human serum, human monocytes, LPS as a challenge) and overall show that metal NPs alone, independent of chemical composition, shape or size, have little capacity to induce innate memory and little capacity to affect the tolerance memory induced by LPS, thereby proving to be generally safe. However, some effects are detectable, which seem to be donor-dependent and exist irrespective of NP characteristics.

2. Results

2.1. Nanoparticle Characterization

Three types of NPs were used in this study: CeO₂ spherical NPs of very small size (CeO₂ SPH, 3.5 nm), stamp-like CeO₂ NPs that shared one dimension with the spherical NP (CeO₂ STA, 3 × 19 nm) and seed-like TiO₂ NPs that shared the other dimension with the stamps (TiO₂ SEE, 19.6 nm) (Figure 1).

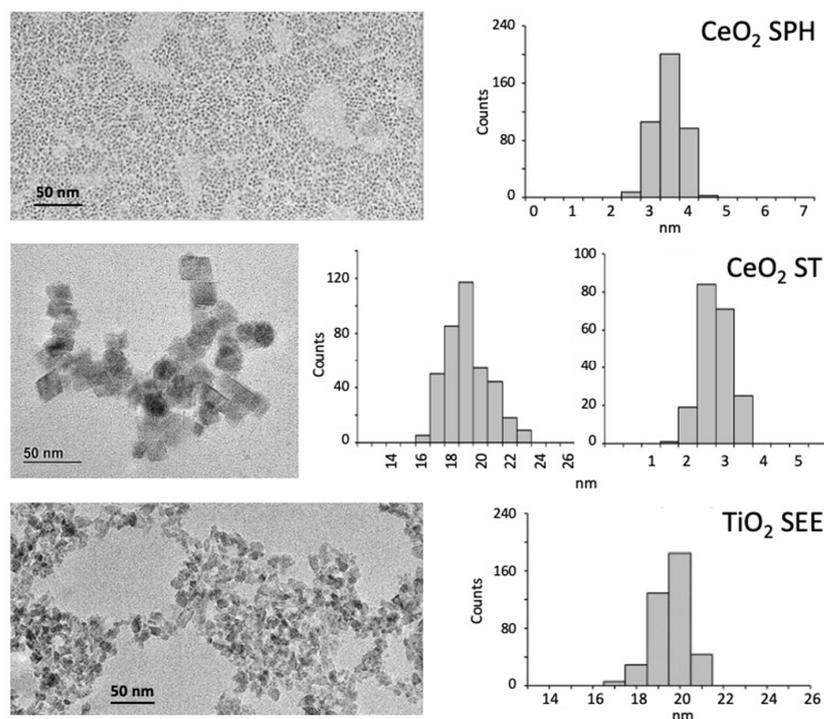


Figure 1. Size and morphology of the NPs used in this study. TEM images (left panels) and TEM number-weighted size distribution (right panels) of spherical CeO₂ NPs (CeO₂ SPH, upper panels), CeO₂ stamp-shaped NPs (CeO₂ STA, middle panels) and TiO₂ seed-shaped NPs (TiO₂ SEE, lower panels). For CeO₂ STA, the distribution of both dimensions (side, thickness) is shown.

The NP morphological characteristics are summarized in Table 1. The NP hydrodynamic features are reported in Table 2 and show that NPs are monodispersed when suspended in their buffer (TMAOH 10 mM), except for CeO₂ SPH that presents two additional peaks of aggregation. Suspension in culture medium leads to significant aggregation in all cases, whereas preincubation of NPs with human serum allows for a good level of dispersion and shows a modest increase in NP hydrodynamic size, attributed to the bio-corona of serum proteins on the NP surface (Table 2). The number-based size distribution shows a similar profile, with serum coating affording good dispersion (Figure S1).

Table 1. Nanoparticle morphology.

Parameter	CeO ₂ SPH	CeO ₂ STA ^a	TiO ₂ SEE
$\langle d \rangle$ (nm)	3.5	19.1, 2.7	19.6
σ_d (nm)	0.4	1.5, 0.4	0.8
$\sigma_d / \langle d \rangle$	9%	13%, 6%	23%
Shape	quasi-sphere	stamp	seed
Stokes diameter (nm) ^b	2.52	38.74	20.52

The mean diameter $\langle d \rangle$ is reported along with the standard deviation of the diameter σ_d and the coefficient of variation $\sigma_d / \langle d \rangle$. ^a Side and thickness ^b by analytical ultracentrifugation.

Table 2. Nanoparticle hydrodynamic features.

Parameter	CeO ₂ SPH	CeO ₂ STA	TiO ₂ SEE
<i>Dh</i> ^a in buffer (nm) ^b	4.2 (37.8) (142) ^c	91.3	68.1
<i>Dh</i> in H ₂ O (nm) ^d	4.2 (28.2) (122)	106	58.8 (5560)
<i>Dh</i> in PBS 1x (nm)	4.2 (28.2) (122)	91.3	58.8 (5560)
<i>Dh</i> in medium (nm) ^e	1480	1110	1480
<i>Dh</i> in medium plus HS (nm) ^f	10.1 (58.8) (459)	190 (5560)	164 (5560)
ζ potential (mV) ^g	−23.60	−40.20	−35.40
Endotoxin activity (EU/mg) ^h	25.0	9.8	4.4

^a *Dh* is the intensity-based hydrodynamic size measured by DLS. ^b Buffer is TMAOH 10 mM for all NP types. ^c Between parentheses is the *Dh* of additional agglomerate peaks in DLS. ^d Endotoxin-free ultrapure water. ^e RPMI-1640 culture medium. ^f NPs precoated with human serum (HS) in RPMI-1640 medium. ^g In PBS 1x. ^h Endotoxin contamination of NP preparations is expressed as activity (endotoxin units, EU) per mg of NPs. All measurements were carried out in triplicate at 25 °C.

A single NP concentration was used for the innate memory experiments. The highest possible endotoxin-free concentration was selected as the working NP concentration. This would allow us to assess NP effects without the confounding presence of strongly inflammatory/activating endotoxin contamination, which would lead to misinterpretation of results. Endotoxin contamination of the NP preparations was measured with an optimized detection assay (Table 2), and NP concentration for the innate memory experiments was adjusted to be at or below 0.01 EU/mL of endotoxin in order to avoid endotoxin-dependent monocyte activation. In fact, human monocytes are highly sensitive to bacterial endotoxin, and even minute amounts of endotoxin (inactive *in vivo* or on other cells *in vitro*) can induce substantial activation. In addition, NP concentration was calculated in order for it to be the same for the three NPs. NP concentration was normalized to total exposed surface area, knowing that, generally, NP interactions with biological systems depend on NP surface area and characteristics. Based on these criteria, the concentration of $2.7 \times 10^7 \mu\text{m}^2$ of total NP surface area/mL was selected, corresponding to 0.5 $\mu\text{g/mL}$ CeO₂ SPH (corresponding to 5.9×10^{12} NPs/mL, with 0.011 EU/mL endotoxin), 1 $\mu\text{g/mL}$ CeO₂ STA (corresponding to 1.5×10^{11} NPs/mL, with 0.010 EU/mL endotoxin) and 1.6 $\mu\text{g/mL}$ TiO₂ SEE (corresponding to 1.2×10^{11} NPs/mL, with 0.007 EU/mL endotoxin). At these concentrations, none of the NPs showed any toxic effect on human monocytes; toxic effect was measured as LDH release after 24 h of exposure and was visually monitored by optical microscopy throughout the entirety of experimental procedures.

2.2. Primary Response of Human Monocytes to LPS and Nanoparticles

Results in Figure 2 show the primary response of human monocytes to NPs alone, to LPS and to LPS admixed with NPs. Production of the inflammatory cytokines TNF α and IL-6 and anti-inflammatory cytokine IL-10 was undetectable in unstimulated cells (exposed for 24 h to culture medium alone; Figure 2A–C), whereas monocytes showed a substantial constitutive production of anti-inflammatory IL-1Ra (light green dotted column in Figure 2D) as expected. Exposure to NPs did not induce production of TNF α , IL-6 and IL-10 and did not change the constitutive IL-1Ra levels. Exposure to LPS induced measurable levels of TNF α , IL-6 and IL-10, while it did not substantially increase the production of IL-1Ra. A quantitative donor-to-donor variability was observed in the response to LPS; thus, the induction of IL-10 by LPS did not reach statistical significance.

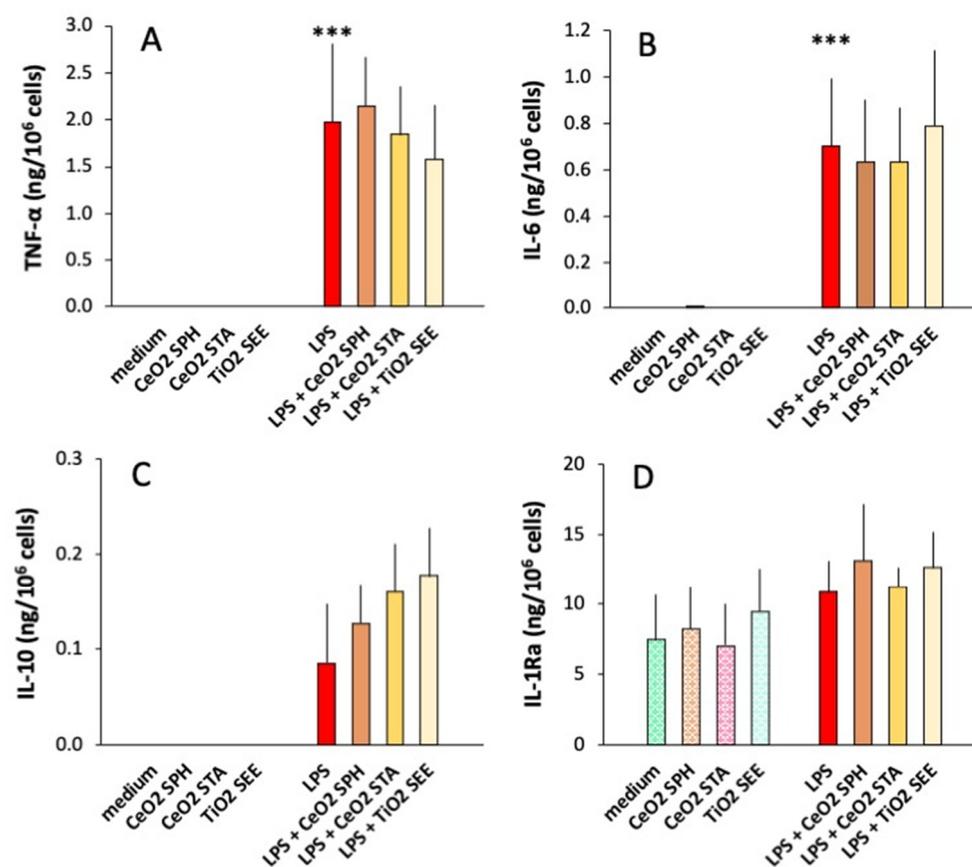


Figure 2. Primary innate immune response of human monocytes to LPS, NPs or their mixture. Human blood monocytes were exposed in culture to medium alone (dotted green columns) or containing 0.5 $\mu\text{g}/\text{mL}$ CeO_2 SPH (dotted orange columns), 1.0 $\mu\text{g}/\text{mL}$ CeO_2 STA (dotted pink columns), or 1.6 $\mu\text{g}/\text{mL}$ TiO_2 SEE (dotted light blue columns), or to 1 ng/mL LPS alone (red columns) or together with NPs (brown, orange and light-yellow columns). The levels of inflammatory ($\text{TNF}\alpha$, IL-6; (A,B)) and anti-inflammatory cytokines (IL-10, IL-1Ra; (C,D)) were measured in the 24 h supernatants by ELISA. The columns represent the average value + SEM from three individual donors. Statistical significance: *** $p < 0.001$, medium (with or without NPs) vs. LPS (with or without NPs) for $\text{TNF}\alpha$ and IL-6; medium vs. LPS for IL-10 and IL-1Ra, medium vs. NPs, and LPS vs. LPS + NPs always not significant.

Co-exposure to LPS and NPs did not change the overall extent of response to LPS, although some individual effects could be observed. The results in Figure 3 show the different behavior of monocytes from two subjects in response to co-exposure to LPS and TiO_2 SEE NPs, with cells of one subject showing a decreased production of $\text{TNF}\alpha$ in the presence of NPs and cells from another subject showing an increase, while the production of IL-10 was increased in both (Figure 3).

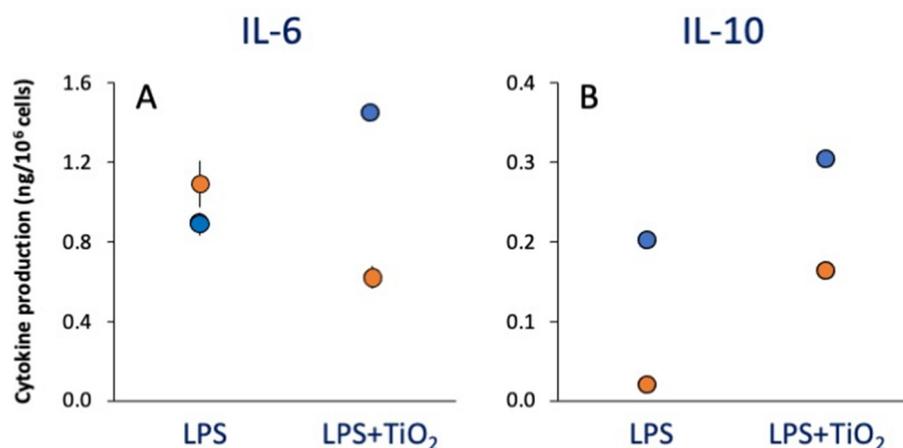


Figure 3. Primary innate immune response of human monocytes from individual donors to LPS, TiO₂ SEE NPs or their mixture. Human blood monocytes from two individual donors (blue and orange dots) were exposed to LPS alone or in the presence of TiO₂ SEE NPs, and the production of inflammatory IL-6 (A) and anti-inflammatory IL-10 (B) was measured after 24 h. Data are the average \pm SD of two replicate determinations. All values of LPS + TiO₂ SEE NPs were significantly different ($p < 0.05$) from values of LPS alone.

2.3. Memory Response of Human Monocytes to LPS and Nanoparticles

After assessing their primary response to NPs, LPS and LPS + NPs, cells were washed and cultured with fresh medium for seven days. This period of time was selected to allow cells to undergo a complete extinction of their activation (as measured by their inability to produce cytokines above the background levels; Figure 4, CTR). In this time frame, cultured monocytes spontaneously differentiate into macrophages. Thus, we can consider them to represent the memory macrophages derived from monocytes recruited to a tissue that has experienced and resolved an infectious event. Figure 4 shows the secondary “memory” response of these macrophages to a challenge with LPS. It should be noted that the LPS concentration used for the challenge is higher than that used for the primary activation. This is meant to mimic a more severe infection so as to assess the efficacy of memory macrophages when reacting to a severe infectious event. Additionally, one should bear in mind that macrophages are generally less reactive than monocytes to microbial stimuli (to avoid excessive reaction to low-level triggering and the associated risk of unwanted tissue damage), and that they are activated towards effector functions only in response to substantial stimulation. Here, we can observe that unprimed cells (medium-primed cells, light green dotted columns) respond to the LPS challenge by producing cytokine levels that are similar to those produced by fresh monocytes in response to a 5x lower LPS concentration, which confirms the notion that macrophages are generally less responsive to challenges. Despite some donor-to-donor variability, the induction of TNF α , IL-6 and IL-10 production in response to LPS was statistically significant (Figure 4A–C), while, as expected, no increase in IL-1Ra production over the substantial constitutive production was observed (Figure 4D). When examining the memory response of NP-primed macrophages (dotted columns), we can observe essentially unchanged overall production of all cytokines relative to medium-primed cells, although again with some donor-to-donor variability. Priming with LPS (red columns) induced a typical tolerance-type memory response, characterized by decreased production of the inflammatory cytokines TNF α and IL-6 but no reduction in the production of the anti-inflammatory factors IL-10 and IL-1Ra.

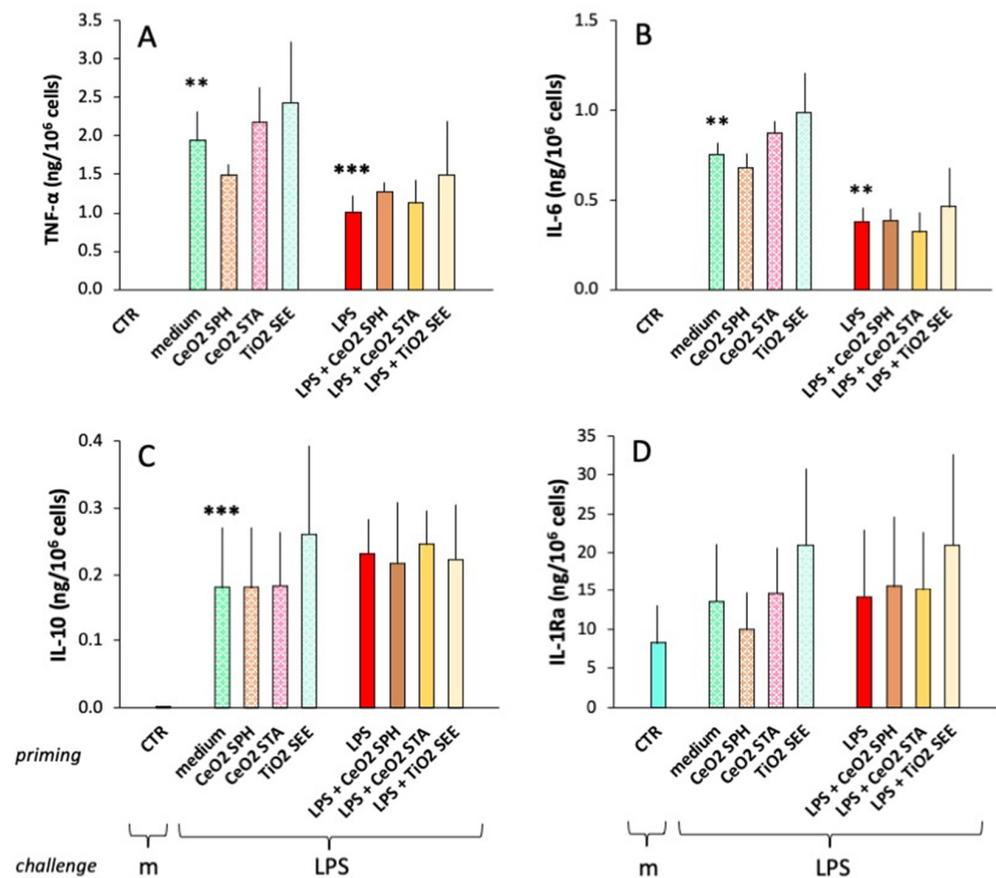


Figure 4. Secondary “memory” response of human monocytes primed with LPS, NPs or their mixture. After a primary exposure to NPs alone or admixed with LPS (see Figure 2; conditions indicated in the “priming” abscissa row), cells were washed and rested in culture for seven days to allow for extinction of primary activation, and then challenged for 24 h with either medium (m in the “challenge” abscissa row) or LPS (LPS in the “challenge” abscissa row). Controls (CTR; light blue columns) include cells primed with medium, buffers, NPs, LPS and LPS + NPs, which are all at baseline (as assessed upon challenge with medium), thereby confirming the complete extinction of primary activation. Inflammatory (TNF α , IL-6; (A,B)) and anti-inflammatory cytokines (IL-10, IL-1Ra; (C,D)) were measured in the 24 h supernatants by ELISA. The columns represent the average value + SEM from three individual donors. Statistical significance: ** $p < 0.01$ unchallenged controls CTR vs. medium-primed LPS-challenged (medium) for TNF α and IL-6, and for medium-primed vs. LPS-primed (LPS) for IL-6; *** $p < 0.001$, medium-primed vs. LPS-primed for TNF α , and CTR vs. medium-primed for IL-10. Other comparisons (CTR vs. medium for IL-1Ra, medium vs. LPS for IL-10 and IL-1Ra, medium vs. NPs, LPS vs. LPS + NPs) not significant.

Overall, co-priming with LPS and NPs did not change the LPS priming effects (decrease in inflammatory TNF α and IL-6 production, unmodified production of anti-inflammatory IL-10 and IL-1Ra), although there were again some donor-to-donor differences. For instance, as shown in Figure 5A, cells from donor 1 (dots) seem to develop a potentiating memory to TiO₂ NP priming in terms of the production of TNF α both alone and upon co-priming with LPS; thus, the reduction in TNF α caused by LPS tolerance (see red dot) is completely reversed in cells primed with LPS and TiO₂ NPs (purple dot). With cells from another donor (squares), while LPS priming induced the expected tolerance-type memory (reduction of TNF α levels), TiO₂ NPs did not induce any kind of memory, as the same level of TNF α was produced by cells primed with medium or with TiO₂ NPs (light blue vs. orange squares) and by cells primed with either LPS or LPS and TiO₂ NPs (red vs. purple squares). Looking at the memory effects on anti-inflammatory IL-10 production (Figure 5B), cells from one donor (dots) displayed low reactivity to the LPS challenge

and showed a potentiating memory response after priming with both TiO₂ NPs and LPS, whereas priming with the combined agents was less effective than either one alone. Cells from the other donor (medium-primed cells, light blue square) showed no effect after priming with TiO₂ NPs, LPS or their combination. Thus, one donor (dots) seemed to develop memory in response to TiO₂ NPs for both inflammatory and anti-inflammatory cytokines, while the combined priming was only effective on TNF α production. Conversely, cells from the other donor seemed unresponsive to TiO₂ NPs in all conditions.

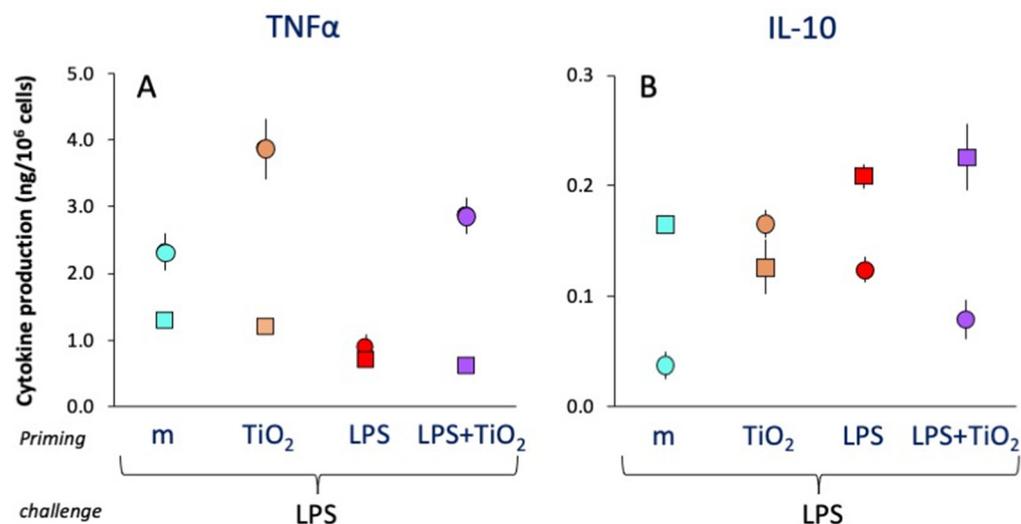


Figure 5. Secondary “memory” response of human monocytes from individual donors primed with LPS, TiO₂ SEE NPs or their mixture. Human blood monocytes from two individual donors (donor 1, dots; donor 2, squares) were primed with medium alone (light blue symbols), LPS (red symbols), TiO₂ SEE NPs (orange symbols) or their mixtures (purple symbols) and then rested and challenged with LPS, as described in Figure 4. The production of inflammatory TNF α (A) and anti-inflammatory IL-10 (B) was measured after 24 h. Data are the average \pm SD of two replicate determinations. Statistical significance: TNF α : $p < 0.05$, m vs. LPS priming (light blue vs. red symbols, both donors), TiO₂ vs. m and LPS + TiO₂ vs. LPS priming in donor 1 (light blue and purple vs. red dots); IL-10: $p < 0.05$, m vs. TiO₂ and LPS priming in donor 1 (light blue vs. orange and red dots). Other comparisons are not significant.

3. Discussion

We have compared the experimental data presented here with results obtained in previous studies performed with other NPs under the same experimental conditions, making them therefore directly comparable. The summary presented in Table 3 shows that innate memory induced by microbial agents is not generally affected by the presence of NPs, independent of their chemical nature (Au, FeOx, CeO₂, TiO₂), size (3–50 nm) or shape (spherical, rod, stamp, seed). The data in Table 3 also confirm the observation of a variability among donors in the NP effects on innate memory, indicated by large average variations vs. control (up to 63%) that do not reach statistical significance.

A number of considerations should be made in order to understand the relevance of these observations. First, the experimental model was designed in order to approximate real-life conditions as much as possible. Thus, human primary cells were used (excluding mouse cells and transformed cell lines), and NPs were used at concentrations in which endotoxin contamination was below functional efficacy (excluding effects not due to NPs) and were pre-exposed to human serum (to reproduce the biocorona formation that occurs when NPs enter the human body). The NP concentrations used (1.0–3.2 $\mu\text{g}/10^6$ monocytes) are in the range expected for intravenous nanodrugs (i.e., about 10 $\mu\text{g}/10^6$ monocytes in blood) and much higher than those foreseen for inhaled/ingested particles.

Table 3. Overall effects of NPs on memory cytokine production induced by microbial agents.

Priming	NPs	Memory TNF α Production		Memory IL-6 Production		Memory IL-10 Production		Memory IL-1Ra Production		N
		Variation vs. No NPs (%)	<i>p</i>	Variation vs. No NPs (%)	<i>p</i>	Variation vs. No NPs (%)	<i>p</i>	Variation vs. No NPs (%)	<i>p</i>	
LPS + NPs	Au 50 nm	−26	<i>ns</i>	nt	<i>nt</i>	nt	<i>nt</i>	nt	<i>nt</i>	4
	Au 12 nm	+35	<i>ns</i>	0	<i>ns</i>	+31	<i>ns</i>	+37	<i>ns</i>	3
	Au ROD	+63	<i>ns</i>	−4	<i>ns</i>	+15	<i>ns</i>	+2	<i>ns</i>	3
	FeOx17	−10	<i>ns</i>	+27	<i>ns</i>	+22	<i>ns</i>	+20	<i>ns</i>	3
	FeOx22	−25	<i>ns</i>	+8	<i>ns</i>	+43	<i>ns</i>	−4	<i>ns</i>	3
	CeO ₂ SPH	+1	<i>ns</i>	+2	<i>ns</i>	+1	<i>ns</i>	+33	<i>ns</i>	3
	CeO ₂ STA	−17	<i>ns</i>	−9	<i>ns</i>	+5	<i>ns</i>	+52	<i>ns</i>	3
TiO ₂ SEE	−19	<i>ns</i>	+25	<i>ns</i>	−8	<i>ns</i>	+24	<i>ns</i>	3	
MDP + NPs	Au 50 nm	−39	<0.05	nt	<i>nt</i>	nt	<i>nt</i>	nt	<i>nt</i>	4
β -glucan + NPs	Au 50 nm	+30	<i>ns</i>	nt	<i>nt</i>	nt	<i>nt</i>	nt	<i>nt</i>	4
<i>H. pylori</i> + NPs	Au 50 nm	0	<i>ns</i>	0	<i>ns</i>	−30	<0.05	+3	<i>ns</i>	12
<i>S. aureus</i> + NPs	Au 50 nm	−4	<i>ns</i>	nt	<i>nt</i>	nt	<i>nt</i>	nt	<i>nt</i>	8
<i>C. albicans</i> + NPs	Au 50 nm	+9	<i>ns</i>	+8	<i>ns</i>	+12	<i>ns</i>	+4	<i>ns</i>	4

The table reports a summary of NP effects of innate memory (assessed as production of inflammatory and anti-inflammatory cytokines) induced in human monocytes by microbial stimuli. LPS priming data are taken from Swartzwelter et al. [61] for spherical 50 nm AuNPs, from Della Camera et al. [63] for spherical 12 nm AuNPs, rod-shaped AuNPs (20 × 13 nm) and spherical FeOx NPs of 17 and 22 nm; data for CeO₂ and TiO₂ NPs are from this study. All other data, with spherical 50 nm AuNPs, are from Swartzwelter et al. [61]. All NPs were used at the maximal endotoxin-free concentration, i.e., 20 μ g/mL for 50 nm AuNPs, 5.7 μ g/mL for 12 nm AuNPs, 1.4 μ g/mL for ROD AuNPs, 2.0 μ g/mL for FeOx17 NPs, 2.7 μ g/mL for FeOx22 NPs, 0.5 μ g/mL for CeO₂ SPH NPs, 1.0 μ g/mL for CeO₂ STA NPs and 1.6 μ g/mL for TiO₂ SEE NPs. After priming, cells were rested in culture for 6–7 days and then challenged with 5–10 ng/mL of LPS. Memory cytokine production was measured after 24 h. NP-dependent variations in memory cytokine production are reported as the percentage of response in cells primed in the absence of NPs and are the average of data from 3–12 donors (donor number N reported in the right column; SD not reported). Variations above (+) and below (−) the values in the absence of NP priming are never statistically significant (*ns* in the *p* columns). A limited but significant decrease was only observed for 50 nm AuNPs in TNF α production in cells primed with the gram-positive bacterial molecule muramyl dipeptide (MDP), suggesting tolerance-type memory (decreased inflammation), and in IL-10 production in cells primed with the gram-negative bacteria *H. pylori*, suggesting a more inflammatory secondary reaction. nt, not tested.

The anti-inflammatory effects of CeO₂ NPs described in several studies [44–49] were not observed here, as CeO₂ NPs did not downregulate LPS-induced inflammatory activation, in line with other studies with human monocytes [64]. It is likely that the anti-inflammatory effects of CeO₂ NPs may be evident at much higher NP concentrations than those used in studies with human primary monocytes. Thus, although the number of donors is low and some variability is observed, these data confirm all the previous data generated with other NPs and suggest that, under “physiological” dose conditions and in the presence of biological fluids, NPs are unable to directly induce an innate immune reaction or modulate a reaction induced by microbial agents, an observation that suggests their general safety.

Innate memory, the immune mechanism that allows for a more protective non-specific reaction to repeated challenges [1–9], was here assessed in terms of the production of two inflammatory cytokines (TNF α and IL-6) and two anti-inflammatory factors (IL-10 and IL-1Ra). Memory induced by priming with LPS is typically characterized by decreased secondary production of inflammatory factors, which aims to reduce the risk of a detrimental secondary inflammatory reaction [10–16]. In this study, tolerance-type innate memory was evident in the decreased production of both TNF α and IL-6, while the production of anti-inflammatory IL-10 and IL-1Ra was unaffected (Figure 4). Thus, the protective memory profile generated in response to LPS priming is represented by decreased inflammation in parallel with unchanged anti-inflammatory mechanisms. We evaluated whether co-exposure to different types of engineered NPs together with LPS interferes with the generation of this putatively protective innate memory profile and showed that NPs of

different chemical composition (CeO_2 , TiO_2) and different shape (spherical, star-like, seed-like) cannot substantially affect the ability of LPS to induce its classical memory profile. This confirms and extends previous studies with NPs of different chemical composition (gold, iron oxide), different size (12, 17, 22, 50 nm) and different shape (spherical, rod-like) (Table 3) [57,60,61,63], and underlines the general safety of NPs not only in terms of direct capacity to induce an innate inflammatory reaction, but also in terms of unwanted induction/modulation of innate memory.

From this study (Figures 3 and 5) and previous results [57,60,61,63], some donor-to-donor variability in reactions to both microbial agents and NPs is evident. The fact that different individuals may develop innate memory in a different fashion, and that NPs may have effects on the microbial-induced innate memory of some individuals but not others, underlines the importance of our personal immunological history, i.e., our “immunobiography”, in determining our immune competence and capacity to react to future challenges [65]. The donor-to-donor variability observed with human subjects is not observed in inbred mice, whose macrophages seem to develop innate memory in response to TLR agonists and NPs without notable interindividual variability [59,66], or with cells from the mouse macrophage-like leukemia cell line RAW 264.7 [66]. Such observations therefore stress the degree of immunological variability in human subjects and emphasize the need for personalized assessment of NP effects on human immunity in view of future nanomedical applications and general nano-immunotoxicity assessments (at least until better knowledge is attained).

Overall, this analysis suggests that NPs may be considered as generally safe from the point of view of innate immune responses as they fail to directly induce cell activation or affect immune activation induced by bacterial molecules such as LPS. However, despite a general lack of effects, the fact NPs can modulate innate memory responses in cells from some subjects suggests caution in the medical use of NPs and the need for personalized NP safety/efficacy profiling.

4. Materials and Methods

4.1. Nanoparticle Synthesis and Characterisation

All synthesis processes were carried out using depyrogenated glassware and reagents were prepared using endotoxin-free water.

The 3.5 nm CeO_2 spheres (CeO_2 SPH) were synthesized by the non-isothermal precipitation procedure based on the method of Zhou et al. [67] and Chen and Chang [68], with some modifications. Briefly, 50 mL of cerium (III) nitrate solution ($\text{Ce}(\text{NO}_3)_3 \cdot 6\text{H}_2\text{O}$) 0.02 M was set at 70 °C with a stirring rate of 500 rpm and then added to 25 mL of 1M tetramethylammonium hydroxide (TMAOH), with the immediate formation of a white precipitate. Incubation was prolonged for 5 min in order to oxidize Ce(III) to Ce(IV). The solution was then rapidly transferred to a water bath, and the reaction continued at 50 °C for 16–18 h. The resulting solution was centrifuged, washed and resuspended in 50 mL 1 mM TMAOH to stabilize the formed 3.5 nm CeO_2 NP.

CeO_2 stamps STA (CeO_2 STA) were synthesized in a similar way to spheres, except that TMAOH was replaced by hexamethylenetetramine (HMT), as described by García et al. [69]. Basically, Ce^{3+} ions from $\text{Ce}(\text{NO}_3)_3$ were oxidized under alkaline pH conditions to Ce^{4+} using HMT. CeO_2 stamp-shaped NPs precipitated and were stabilized in water with HMT, which forms a double electrical layer to prevent NP aggregation.

For titanium dioxide seed-shaped NPs (TiO_2 SEE), the synthesis procedure was based on Pottier et al. [70]. Titanium tetrachloride (TiCl_4) was decomposed at an acidic pH (from 2 to 6), and the growth of the nanocrystals was then carried out in an oven at 70 °C. Finally, a purification step involving centrifugation and re-suspension with TMAOH was used to stabilize the NP dispersion.

NP characterization images were obtained by STEM (scanning transmission electron microscopy) using an FEI Magellan XHR microscope (FEI, Hillsboro, OR, USA) in transmission mode with an acceleration of 20 kV. Particle size was assessed using an ImageJ macro.

Particle ζ -potential and hydrodynamic diameter were determined by laser doppler velocimetry and dynamic light scattering (DLS), respectively, using a Malvern Zetasizer Nano ZS instrument (Malvern Panalytical Ltd., Malvern, UK) with a light source wavelength of 632.8 nm and a fixed scattering angle of 173° (at 25°C).

For all NP types, the main physico-chemical characteristics are reported in Figure 1 and Tables 1 and 2. All NPs were pre-coated with human AB serum (Merck Sigma-Aldrich[®], St. Louis, MO, USA) immediately before use in monocyte stimulation experiments. Briefly, NP suspensions were admixed 1:1 with heat-inactivated serum and incubated for 2 h at 37°C in an orbital shaker at 500 rpm. NPs were then diluted in culture medium to the concentration required for use in the biological assays, and serum concentration was adjusted to 5%. Coating with serum significantly increased the colloidal stability of all NPs (Table 2 and Figure S1).

4.2. Human Monocyte Isolation

Blood was obtained from healthy donors after obtaining informed consent in accordance with the Declaration of Helsinki. The protocol was approved by the Regional Ethics Committee for Clinical Experimentation of the Tuscany Region (Ethics Committee Register n. 14,914 of 16 May 2019).

Monocytes were isolated by CD14 positive selection with magnetic microbeads (Miltenyi Biotec, Bergisch Gladbach, Germany) from peripheral blood mononuclear cells (PBMC), obtained by Ficoll-Paque gradient density separation (GE Healthcare, Bio-Sciences AB, Uppsala, Sweden). The monocyte preparations used in the experiments were $>95\%$ viable and $>95\%$ pure (assessed by trypan blue exclusion and cytosmeears). Monocytes isolated with this method were not activated, based on analysis of the expression of inflammation-related genes (*IL1B*, *TNFA*) and the release of encoded proteins, compared to monocytes within PBMC (i.e., after Ficoll-Paque separation) and whole blood (i.e., after withdrawal with anticoagulants).

Monocytes were cultured in culture medium (RPMI 1640 + Glutamax-I; GIBCO by Life Technologies, Paisley, UK) supplemented with $50\ \mu\text{g}/\text{mL}$ gentamicin sulfate (GIBCO) and 5% heat-inactivated human AB serum (Merck Sigma-Aldrich[®]). Cells (5×10^5) were seeded at a final volume of 1.0 mL in the wells of 24-well flat bottom plates (Corning[®] Costar[®]; Corning Inc. Life Sciences, Oneonta, NY, USA) at 37°C in moist air with 5% CO_2 . Monocyte stimulation was performed after resting overnight.

4.3. Human Monocyte Activation and Induction of Innate Memory

For assessing the primary response to stimulation, monocytes were exposed for 24 h to culture medium alone (medium/negative control) or medium containing $1\ \text{ng}/\text{mL}$ LPS (positive control; from *E. coli* O55:B5; Merck Sigma-Aldrich[®]), serum pre-coated NPs or LPS together with NPs.

For memory experiments, after the first exposure to stimuli for 24 h and supernatant collection, cells were washed and cultured with fresh culture medium for 7 additional days (one medium change after 4 days). During this period, the activation induced by previous stimulation subsides, and cells return to their baseline status (as determined by evaluation of inflammation-related cytokines in the supernatant). After the resting phase, the supernatant was collected, and cells were challenged for 24 h with fresh medium alone or medium containing $5\ \text{ng}/\text{mL}$ LPS (at a $5\times$ higher concentration than in the primary stimulation to mimic a stronger secondary challenge).

All supernatants (collected after the first stimulation, after the resting phase and after the challenge phase) were frozen at -20°C for subsequent cytokine analysis. By visual inspection, cell viability and cell number did not substantially change in response to the different treatments.

4.4. Cytotoxicity Evaluation

The direct toxicity of NPs on monocytes was evaluated through the release of lactate dehydrogenase (LDH). Briefly, monocytes (1.2×10^5 cells/well of 96-well plates; Corn-

ing Inc., Corning, NY, USA) were incubated for 24 h in 200 μ L of culture medium alone or medium containing serum-coated NPs in triplicate. Positive control wells received 200 μ L of 0.1% Triton-X 100. At the end of the incubation, release of the cytoplasmic enzyme LDH was measured in the supernatant using a colorimetric assay (LDH-Cytotoxicity Colorimetric Assay Kit; BioVision, Inc., Milpitas, CA, USA). Validation of the LDH cytotoxicity results was obtained by visual inspection of cells in culture over the entire course of the experiments. Cell density (variations in the number of cells in culture), cell refractivity, morphology and adherence (associated to live/dead cells) were assessed by phase contrast optical microscopy at 24 h (after the first stimulus), 8 days (after the resting period) and at 9 days (after the challenge).

4.5. Assessment of Endotoxin Contamination

Endotoxin contamination in NPs was assessed with a commercial chromogenic Limulus Amoebocyte Lysate (LAL) assay (Pyros Kinetix[®] Flex; Associates of Cape Cod, Inc., East Falmouth, MA, USA) following a protocol adapted for use with particulate agents [71]. Preliminary controls were run to assess the possible interference of NPs in the assay readout. These encompassed direct optical reading at 405 nm (the OD of the assay readout product paranitroaniline, pNA) and interference with detection of different concentrations of synthetic pNA. NPs were used in the LAL assay at concentrations that did not interfere with the assay readout. Additional controls included assessment of the possible interference of NPs with the assay components/reagents, performed by spiking the NP samples with a known amount of LPS (0.5 EU/mL) and assessing the recovery of spiked endotoxin. A recovery rate between 80 and 120% was considered acceptable. The endotoxin contamination was therefore reliably assessed at NP dilutions that did not interfere with the 405 nm readout and in which 80–120% spiked endotoxin could be recovered. The LAL assay was run with Glucashield[®] (Associates of Cape Cod, Inc.) using a dedicated tube reader and software (Associates of Cape Cod, Inc.) to eliminate possible false positives due to the presence of glucans. Assay sensitivity was 0.001 EU/mL.

4.6. Evaluation of Cytokine Production

The levels of the human inflammatory cytokines TNF α and IL-6 and anti-inflammatory factors IL-10 and IL-1Ra produced by cultured monocytes were assessed in cell supernatants by ELISA (R&D Systems, Minneapolis, MN, USA) using a Cytation 3 imaging multi-mode reader (BioTek, Winooski, VT, USA). The presence of IL-1 β was not measured because, from preliminary experiments, the production of this inflammatory cytokine in cells challenged with LPS after primary activation and 7 days of resting was below detection even in controls. Each sample was tested in duplicate in ELISA.

4.7. Statistical Analysis

Data were analyzed using GraphPad Prism6.01 software (GraphPad Inc., La Jolla, CA, USA). For cytokine production, results are presented as ng of produced cytokine/ 10^6 plated monocytes. Results are reported as the mean of values from three donors, each tested with two to six replicates. The statistical significance of differences is indicated by *p* values, which were calculated with unpaired and two-tailed Student's *t*-tests.

Supplementary Materials: The supporting information can be downloaded at: <https://www.mdpi.com/article/10.3390/ijms232314655/s1>.

Author Contributions: D.B. wrote the manuscript; G.D.C. performed the experimental work and the analytical NP characterization; T.L. and W.Y. analyzed the data; V.F.P. synthesized and characterized the NPs; D.B., Y.L., S.G. and P.I. contributed to the experimental design; all authors critically revised the manuscript. All authors have read and agreed to the published version of the manuscript.

Funding: This work was supported by the EU Commission H2020 projects PANDORA (GA671881) and ENDONANO (GA 812661) (PI, DB), the Italian MIUR InterOmics Flagship projects MEMORAT and MAME (DB, PI), and the Presidential International Fellowship Program (PIFI) of the Chinese

Academy of Science (2020VBA0028) (DB). Part of this work was carried out in the context of the JRC Visiting Scientist agreement no. 05/JRC.F.2/2019 (Directorate F—Health, Consumers and Reference Materials, Consumer Products Safety, Nanobiotechnology Lab).

Institutional Review Board Statement: The study was conducted in accordance with the Declaration of Helsinki and approved by the Regional Ethics Committee for Clinical Experimentation of the Tuscany Region (Ethics Committee Register n. 14,914 of 16 May 2019).

Informed Consent Statement: Informed consent was obtained from all subjects involved in the study.

Data Availability Statement: Data supporting reported results can be found in the supplementary material and are available from the authors upon request.

Acknowledgments: We are grateful to Giuliana Donini, who has continuously encouraged and supported our studies. We thank Paola Migliorini (University of Pisa) for the ethical monitoring of our studies with human blood cells, Jessica Ponti (JRC) for TEM support, and Dora Mehn (JRC), Ben Swartzwelter (University of Colorado, Denver, CO, USA) and Jutta Horejs-Hoeck (Paris-Lodron University of Salzburg, Austria) for helpful discussion. DB also wishes to thank Wang Rui for her relentless efforts in facilitating our scientific work.

Conflicts of Interest: The authors declare no conflict of interest. The funders had no role in the design of the study; in the collection, analyses or interpretation of data; in the writing of the manuscript; or in the decision to publish the results.

References

1. Kurtz, J. Specific memory within innate immune systems. *Trends Immunol.* **2005**, *26*, 186–192. [[CrossRef](#)] [[PubMed](#)]
2. Foster, S.L.; Hargreaves, D.C.; Medzhitov, R. Gene-specific control of inflammation by TLR-induced chromatin modifications. *Nature* **2007**, *447*, 972–978. [[CrossRef](#)] [[PubMed](#)]
3. Netea, M.G.; Quintin, J.; van der Meer, J.W. Trained immunity: a memory for innate host defense. *Cell Host Microbe* **2011**, *9*, 355–361. [[CrossRef](#)] [[PubMed](#)]
4. Netea, M.G.; Joosten, L.A.; Latz, E.; Mills, K.H.; Natoli, G.; Stunnenberg, H.G.; O'Neill, L.A.; Xavier, R.J. Trained immunity: a program of innate immune memory in health and disease. *Science* **2016**, *352*, aaf1098. [[CrossRef](#)]
5. Sun, J.C.; Ugolini, S.; Vivier, E. Immunological memory within the innate immune system. *EMBO J.* **2014**, *33*, 1295–1303. [[CrossRef](#)]
6. Milutinovic, B.; Kurtz, J. Immune memory in invertebrates. *Semin. Immunol.* **2016**, *28*, 328–342. [[CrossRef](#)]
7. Reimer-Michalski, E.M.; Conrath, U. Innate immune memory in plants. *Semin. Immunol.* **2016**, *28*, 319–327. [[CrossRef](#)]
8. Melillo, D.; Marino, R.; Italiani, P.; Boraschi, D. Innate immune memory in invertebrate metazoans: a critical appraisal. *Front. Immunol.* **2018**, *9*, 1915. [[CrossRef](#)]
9. Pradeau, T.; Du Pasquier, L. Immunological memory: what's in a name? *Immunol. Rev.* **2018**, *283*, 7–20. [[CrossRef](#)]
10. Beeson, P.B. Development of tolerance to typhoid bacterial pyrogen and its abolition by reticulo-endothelial blockade. *Proc. Soc. Exp. Biol. Med.* **1946**, *61*, 248–250. [[CrossRef](#)]
11. Dubos, R.J.; Schaedler, R.W. Reversible changes in the susceptibility of mice to bacterial infections. I. Changes brought about by injection of pertussis vaccine or of bacterial endotoxins. *J. Exp. Med.* **1956**, *104*, 53–65. [[CrossRef](#)]
12. Fan, H.; Cook, J.A. Molecular mechanisms of endotoxin tolerance. *J. Endotoxin Res.* **2004**, *10*, 71–84. [[CrossRef](#)] [[PubMed](#)]
13. Cavaillon, J.-M.; Adib-Conquy, M. Bench-to-bedside review: endotoxin tolerance as a model of leukocyte reprogramming in sepsis. *Crit. Care* **2006**, *10*, 233. [[CrossRef](#)]
14. Buckley, J.M.; Wang, J.H.; Redmond, H.P. Cellular reprogramming by Gram-positive bacterial components: a review. *J. Leukoc. Biol.* **2006**, *80*, 731–741. [[CrossRef](#)] [[PubMed](#)]
15. Morris, M.C.; Gilliam, E.A.; Li, L. Innate immune programming by endotoxin and its pathological consequences. *Front. Immunol.* **2014**, *5*, 680. [[CrossRef](#)] [[PubMed](#)]
16. Seeley, J.J.; Ghosh, S. Molecular mechanisms of innate memory and tolerance to LPS. *J. Leukoc. Biol.* **2017**, *101*, 107–119. [[CrossRef](#)]
17. Boehme, D.; Dubos, R.J. The effect of bacterial constituents on the resistance of mice to heterologous infection and on the activity of their reticuloendothelial system. *J. Exp. Med.* **1958**, *107*, 523–536. [[CrossRef](#)]
18. Bistoni, F.; Vecchiarelli, A.; Cenci, E.; Puccetti, P.; Marconi, P.; Cassone, A. Evidence for macrophage-mediated protection against lethal *Candida albicans* infection. *Infect. Immun.* **1986**, *51*, 668–674. [[CrossRef](#)]
19. Bowdish, D.M.E.; Loffredo, M.S.; Mukhopadhyay, S.; Mantovani, A.; Gordon, S. Macrophage receptors implicated in the “adaptive” form of innate immunity. *Microbes Infect.* **2007**, *9*, 1680–1687. [[CrossRef](#)]
20. Sun, J.C.; Beilke, J.N.; Lanier, L.L. Immune memory redefined: characterizing the longevity of natural killer cells. *Immunol. Rev.* **2010**, *236*, 83–94. [[CrossRef](#)]
21. O'Sullivan, T.E.; Sun, J.C.; Lanier, L.L. Natural killer cell memory. *Immunity* **2015**, *43*, 634–645. [[CrossRef](#)] [[PubMed](#)]

22. Martinez-Gonzalez, I.; Math, L.; Steer, C.A.; Takei, F. Immunological memory of group 2 innate lymphoid cells. *Trends Immunol.* **2017**, *38*, 423–431. [[CrossRef](#)] [[PubMed](#)]
23. Serafini, N.; Jarade, A.; Surace, L.; Goncalves, P.; Sismeiro, O.; Varet, H.; Legendre, R.; Coppee, J.Y.; Disson, O.; Durum, S.K.; et al. Trained ILC3 responses promote intestinal defense. *Science* **2022**, *375*, 859–863. [[CrossRef](#)] [[PubMed](#)]
24. Naik, S.; Larsen, S.B.; Gomez, N.C.; Alaverdyan, K.; Sendoel, A.; Yuan, S.; Polak, L.; Kulukian, A.; Chai, S.; Fuchs, E. Inflammatory memory sensitizes skin epithelial stem cells to tissue damage. *Nature* **2017**, *550*, 475–480. [[CrossRef](#)] [[PubMed](#)]
25. Dai, X.; Medzhitov, R. Inflammation: memory beyond immunity. *Nature* **2017**, *550*, 460–461. [[CrossRef](#)]
26. Nasrollahi, S.; Walter, C.; Loza, A.J.; Schimizzi, G.V.; Longmore, G.D.; Pathak, A. Past matrix stiffness primes epithelial cells and regulates their future collective migration through a mechanical memory. *Biomaterials* **2017**, *146*, 146–155. [[CrossRef](#)]
27. Cassone, A. The case of an expanded concept of trained immunity. *mBio* **2018**, *9*, e00570-18. [[CrossRef](#)]
28. Bigot, J.; Guillot, L.; Guitard, J.; Ruffin, M.; Corvol, H.; Chignard, M.; Hennequin, C.; Balloy, V. Respiratory epithelial cells can remember infection: a proof-of-concept study. *J. Infect. Dis.* **2020**, *221*, 1000–1005. [[CrossRef](#)]
29. Madej, M.; Töpfer, E.; Boraschi, D.; Italiani, P. Different regulation of interleukin-1 production and activity in monocytes and macrophages: innate memory as an endogenous mechanism of IL-1 inhibition. *Front. Pharmacol.* **2017**, *8*, 335. [[CrossRef](#)]
30. Feuerstein, R.; Forde, A.J.; Lohrmann, F.; Kolter, J.; Ramirez, N.J.; Zimmermann, J.; de Agüero, M.G.; Henneke, P. Resident macrophages acquire innate immune memory in staphylococcal skin infection. *eLife* **2020**, *9*, e55602. [[CrossRef](#)]
31. Boraschi, D.; Duschl, A. *Nanoparticles and the Immune System: Safety and Effects*; Academic Press: Oxford, UK, 2013.
32. Mohajerani, A.; Burnett, L.; Smith, J.V.; Kurmus, H.; Milas, J.; Arulrajah, A.; Horpibulsuk, S.; Abdul Kadir, A. Nanoparticles in construction materials and other applications, and implications of nanoparticle use. *Materials* **2019**, *12*, 3052. [[CrossRef](#)] [[PubMed](#)]
33. Shi, H.; Magaye, R.; Castranova, V.; Zhao, J. Titanium dioxide nanoparticles: a review of current toxicological data. *Part. Fibre Toxicol.* **2013**, *10*, 15. [[CrossRef](#)] [[PubMed](#)]
34. Smolkova, B.; El Yamani, N.; Collins, A.R.; Gutleb, A.C.; Dusinska, M. Nanoparticles in food. Epigenetic changes induced by nanomaterials and possible impact on health. *Food Chem. Toxicol.* **2015**, *77*, 64–73. [[CrossRef](#)] [[PubMed](#)]
35. SCCS. *Opinion on Titanium Dioxide (Nano Form) as UV-Filter in Sprays, Preliminary Version of 7 March 2017, Final Version of 19 January 2018*; SCCS/1583/17; SCCS: Brussels, Belgium, 2018.
36. Dréno, B.; Alexis, A.; Chuberre, B.; Marinovich, M. Safety of titanium dioxide nanoparticles in cosmetics. *J. Eur. Acad. Dermatol. Venereol.* **2019**, *33*, 34–46. [[CrossRef](#)]
37. EFSA. Titanium Dioxide: E171 No Longer Considered Safe when Used as a Food Additive. 2021. Available online: <https://www.efsa.europa.eu/en/news/titanium-dioxide-e171-no-longer-considered-safe-when-used-food-additive> (accessed on 3 September 2022).
38. Corma, A.; Atienzar, P.; Garcia, H.; Chane-Ching, J.-Y. Hierarchically mesostructured doped CeO₂ with potential for solar-cell use. *Nat. Mater.* **2004**, *3*, 394–397. [[CrossRef](#)]
39. Reed, K.; Cormack, A.; Kulkarni, A.; Mayton, M.; Sayle, D.; Klaessig, F.; Stadler, B. Exploring the properties and applications of nanoceria: is there still plenty of room at the bottom? *Environ. Sci. Nano* **2014**, *1*, 390–405. [[CrossRef](#)]
40. Ivanov, V.K.; Shcherbakov, A.; Usatenko, A. Structure-sensitive properties and biomedical applications of nanodisperse cerium dioxide. *Russ. Chem. Rev.* **2009**, *78*, 855–871. [[CrossRef](#)]
41. Jung, H.; Kittelson, D.B.; Zachariah, M.R. The influence of a cerium additive on ultrafine diesel particle emissions and kinetics of oxidation. *Combust. Flame* **2005**, *142*, 276–288. [[CrossRef](#)]
42. Campbell, C.T. Oxygen vacancies and catalysis on ceria surfaces. *Science* **2005**, *309*, 713–714. [[CrossRef](#)]
43. Charbgo, F.; Ramezani, M.; Darroudi, M. Bio-sensing applications of cerium oxide nanoparticles: advantages and disadvantages. *Biosens. Bioelectron.* **2017**, *96*, 33–43. [[CrossRef](#)]
44. Chen, J.P.; Patil, S.; Seal, S.; McGinnis, J.F. Rare earth nanoparticles prevent retinal degeneration induced by intracellular peroxides. *Nat. Nanotechnol.* **2006**, *1*, 142–150. [[CrossRef](#)] [[PubMed](#)]
45. Hirst, S.; Karakoti, A.; Tyler, R.; Sriranganathan, N.; Seal, S.; Reilly, C. Anti-inflammatory properties of cerium oxide nanoparticles. *Small* **2009**, *5*, 2848–2856. [[CrossRef](#)] [[PubMed](#)]
46. Colon, J.; Hsieh, N.; Ferguson, A.; Kupelian, P.; Seal, S.; Jenkins, D.W.; Baker, C.H. Cerium oxide nanoparticles protect gastrointestinal epithelium from radiation-induced damage by reduction of reactive oxygen species and upregulation of superoxide dismutase 2. *Nanomedicine* **2010**, *6*, 698–705. [[CrossRef](#)] [[PubMed](#)]
47. DeCoteau, W.; Heckman, K.; Estevez, A.; Reed, K.; Costanzo, W.; Sandford, D.; Studlack, P.; Clauss, J.; Nichols, E.; Lipps, J.; et al. Cerium oxide nanoparticles with antioxidant properties ameliorate strength and prolong life in mouse model of amyotrophic lateral sclerosis. *Nanomedicine* **2016**, *12*, 2311–2320. [[CrossRef](#)] [[PubMed](#)]
48. Kim, J.; Hong, G.; Mazaleuskaya, L.; Hsu, J.C.; Rosario-Berrios, D.N.; Grosser, T.; Cho-Park, P.F.; Cormode, D.P. Ultrasmall antioxidant cerium oxide nanoparticles for regulation of acute inflammation. *ACS Appl. Mater. Interfaces* **2021**, *13*, 60852–60864. [[CrossRef](#)] [[PubMed](#)]
49. Casals, G.; Perramón, M.; Casals, E.; Portolés, I.; Fernández-Varo, G.; Morales-Ruiz, M.; Puentes, V.; Jiménez, W. Cerium oxide nanoparticles: a new therapeutic tool in liver diseases. *Antioxidants* **2021**, *10*, 660. [[CrossRef](#)] [[PubMed](#)]
50. Pelclova, D.; Navratil, T.; Kacerova, T.; Zamostna, B.; Fenclova, Z.; Vlckova, S.; Kacer, P. NanoTiO₂ sunscreen does not prevent systemic oxidative stress caused by UV radiation and a minor amount of nanoTiO₂ is absorbed in humans. *Nanomaterials* **2019**, *9*, 888. [[CrossRef](#)]

51. Baroli, B.; Ennas, M.G.; Loffredo, F.; Isola, M.; Pinna, R.; Lopez-Quintela, M.A. Penetration of metallic nanoparticles in human full-thickness skin. *J. Investig. Dermatol.* **2007**, *127*, 1701–1712. [[CrossRef](#)]
52. Brun, E.; Barreau, F.; Veronesi, G.; Fayard, B.; Sorieul, S.; Chaneac, C.; Carapito, C.; Rabilloud, T.; Mabondzo, A.; Herlin-Boime, N.; et al. Titanium dioxide nanoparticle impact and translocation through ex vivo, in vivo and in vitro gut epithelia. *Part. Fibre Toxicol.* **2014**, *11*, 13. [[CrossRef](#)]
53. Cronin, J.G.; Jones, N.; Thornton, C.A.; Jenkins, G.J.S.; Doak, S.H.; Clift, M.J.D. Nanomaterials and innate immunity: a perspective of the current status in nanosafety. *Chem. Res. Toxicol.* **2020**, *33*, 1061–1073. [[CrossRef](#)]
54. Himly, M.; Geppert, M.; Hofer, S.; Hofstaetter, N.; Horejs-Hoeck, J.; Duschl, A. When would immunologists consider a nanomaterial to be safe? Recommendations for planning studies on nanosafety. *Small* **2020**, *16*, e1907483. [[CrossRef](#)] [[PubMed](#)]
55. Boraschi, D.; Italiani, P.; Palomba, R.; Decuzzi, P.; Duschl, A.; Fadeel, B.; Moghimi, S.M. Nanoparticles and innate immunity: new perspectives on host defence. *Semin. Immunol.* **2017**, *34*, 33–51. [[CrossRef](#)] [[PubMed](#)]
56. Boraschi, D.; Alijagic, A.; Auguste, M.; Barbero, F.; Ferrari, E.; Hernadi, S.; Mayall, C.; Michelini, S.; Navarro Pacheco, N.I.; Prinelli, A.; et al. Addressing nanomaterial immunosafety by evaluating innate immunity across living species. *Small* **2020**, *16*, e2000598. [[CrossRef](#)] [[PubMed](#)]
57. Italiani, P.; Boraschi, D. Induction of innate immune memory by engineered nanoparticles, a hypothesis that may become true. *Front. Immunol.* **2017**, *8*, 734. [[CrossRef](#)]
58. Italiani, P.; Della Camera, G.; Boraschi, D. Induction of innate immune memory by engineered nanoparticles in monocytes/macrophages: from hypothesis to reality. *Front. Immunol.* **2020**, *11*, 566309. [[CrossRef](#)]
59. Lebre, F.; Boland, J.B.; Gouveia, P.; Gorman, A.L.; Lundahl, M.L.E.; Lynch, R.I.; O'Brien, F.J.; Coleman, J.; Lavelle, E.C. Pristine graphene induces innate immune training. *Nanoscale* **2020**, *12*, 11192–11200. [[CrossRef](#)]
60. Swartzwelter, B.J.; Barbero, F.; Verde, A.; Mangini, M.; Pirozzi, M.; De Luca, A.C.; Puentes, V.F.; Leite, L.C.; Italiani, P.; Boraschi, D. Gold nanoparticles modulate BCG-induced innate immune memory in human monocytes by shifting the memory response towards tolerance. *Cells* **2020**, *9*, 284. [[CrossRef](#)]
61. Swartzwelter, B.J.; Michelini, S.; Frauenlob, T.; Barbero, F.; Verde, A.; De Luca, A.C.; Puentes, V.; Duschl, A.; Horejs-Hoeck, J.; Italiani, P.; et al. Innate memory reprogramming by gold nanoparticles depends on the microbial agents that induce memory. *Front. Immunol.* **2021**, *12*, 751683. [[CrossRef](#)]
62. Barbosa, M.M.F.; Kanno, A.I.; Paiva Farias, L.; Madej, M.; Sipos, G.; Sbrana, S.; Romani, L.; Boraschi, D.; Leite, L.C.; Italiani, P. Primary and memory response of human monocytes to vaccines: role of nanoparticulate antigens in inducing innate memory. *Nanomaterials* **2021**, *11*, 931. [[CrossRef](#)]
63. Della Camera, G.; Madej, M.; Ferretti, A.M.; La Spina, R.; Li, Y.; Corteggio, A.; Heinzl, T.; Swartzwelter, B.J.; Sipos, G.; Gioria, S.; et al. Personalised profiling of innate immune memory induced by nano-imaging particles in human monocytes. *Front. Immunol.* **2021**, *12*, 692165. [[CrossRef](#)]
64. Hussain, S.; Al-Nsour, F.; Rice, A.B.; Marshburn, J.; Ji, Z.; Zink, J.I.; Yingling, B.; Walker, N.J.; Garantziotis, S. Cerium dioxide nanoparticles do not modulate the lipopolysaccharide-induced inflammatory response in human monocytes. *Int. J. Nanomed.* **2012**, *7*, 1387–1397. [[CrossRef](#)] [[PubMed](#)]
65. Franceschi, C.; Salvioli, S.; Garagnani, P.; de Eguileor, M.; Monti, D.; Capri, M. Immunobiography and the heterogeneity of immune responses in the elderly: a focus on inflammaging and trained immunity. *Front. Immunol.* **2017**, *8*, 982. [[CrossRef](#)] [[PubMed](#)]
66. Pan, Y.; Li, J.; Xia, X.; Wang, J.; Jiang, Q.; Yang, J.; Dou, H.; Liang, H.; Li, K.; Hou, Y. β -glucan-coupled superparamagnetic iron oxide nanoparticles induce trained immunity to protect mice against sepsis. *Theranostics* **2022**, *12*, 675–688. [[CrossRef](#)] [[PubMed](#)]
67. Zhou, X.D.; Huebner, W.; Anderson, H.U. Room-temperature homogeneous nucleation synthesis and thermal stability of nanometer single crystal CeO₂. *Appl. Phys. Lett.* **2002**, *80*, 3814–3816. [[CrossRef](#)]
68. Chen, H.I.; Chang, H.Y. Synthesis and characterization of nanocrystalline cerium oxide powders by two-stage non-isothermal precipitation. *Solid State Commun.* **2005**, *133*, 593–598. [[CrossRef](#)]
69. García, A.; Delgado, L.; Torà, J.A.; Caslas, E.; González, E.; Puentes, V.; Font, X.; Carrera, J.; Sánchez, A. Effect of cerium dioxide, titanium dioxide, silver, and gold nanoparticles on the activity of microbial communities intended in wastewater treatment. *J. Hazard Mater.* **2012**, *199–200*, 64–72. [[CrossRef](#)] [[PubMed](#)]
70. Pottier, A.; Cassaignon, S.; Chanéac, C.; Villain, F.; Tronca, E.; Jolivet, J.-P. Size tailoring of TiO₂ anatase nanoparticles in aqueous medium and synthesis of nanocomposites. Characterization by Raman spectroscopy. *J. Mater. Chem.* **2003**, *13*, 877–882. [[CrossRef](#)]
71. Li, Y.; Italiani, P.; Casals, E.; Tran, N.; Puentes, V.F.; Boraschi, D. Optimising the use of commercial LAL assays for the analysis of endotoxin contamination in metal colloids and metal oxide nanoparticles. *Nanotoxicology* **2015**, *9*, 462–473. [[CrossRef](#)]